Available online at www.sciencedirect.com
ScienceDirect
Polymer 49 (2008) 867–876
polymer
www.elsevier.com/locate/polymer

Boehmite-based polyethylene nanocomposites prepared by in-situ polymerization

Tobias S. Halbach, Rolf Mülhaupt*

Freiburger Materialforschungszentrum, Institut für Makromolekulare Chemie, Albert-Ludwigs University, Stefan-Meier-Str. 31, 79104 Freiburg, Germany

Received 7 September 2007; received in revised form 27 November 2007; accepted 7 December 2007
Available online 28 January 2008

Abstract

Polyethylene (PE)–boehmite nanocomposites were prepared by means of metallocene/MAO-catalyzed in-situ polymerization of ethylene in the presence of boehmites, which were rendered organophilic by modification with carboxylic acids such as stearic acid and undecylenic acid. Such organoboehmites are readily dispersed in the polymerization media such as toluene. Polymerization activity, filler dispersion and mechanical properties of the nanocomposites were investigated as a function of type and concentration of the organoboehmites. The catalyst activity of different metallocenes (Cp_2ZrCl_2 and *rac*-Me_2Si(2-Me-benz[*e*]-Ind)$_2ZrCl_2$) was increased up to 100% in the presence of organoboehmite fillers. The dispersion of nanoboehmites, as evidenced by TEM studies, was dependent upon the content of the carboxylate modifier. At 20 wt.% carboxylate content uniform dispersions of organoboehmite particles with average particle sizes smaller than 100 nm were obtained. According to stress–strain measurements, the Young's modulus increased with increasing boehmite content without sacrificing high elongation at break.

Keywords: Boehmite; Polyethylene; in-situ polymerization

1. Introduction

The dispersion of inorganic nanoparticles in polymer matrices affords novel materials with improved mechanical properties [1], thermal stability [2], flame retardancy [3,4], chemical resistance, higher barrier properties [5], scratch resistance [6] and ion conductivity [7]. In comparison to conventional micrometer-scaled fillers, the same volume fraction of nanometer-scaled fillers contains nine orders of magnitude higher content of filler particles with much higher surface area. As a consequence, in nanocomposites, most polymers are located at the nanofiller interfaces. When nanoparticles are added bulk polymers are converted into interfacial polymers exhibiting different properties [1,4]. Due to their low percolation threshold, small amounts of just a few percent of nanoparticle additives are sufficient to account for major changes in polymer properties. Strong interactions between nanoparticles are well known to cause formation of nanoparticle agglomerates which can initiate premature mechanical failure when nanocomposites are exposed to external mechanical stresses. The full potential of nanocomposites is only exploited when nanofillers are homogeneously dispersed within the polymer matrix [1].

Nanocomposites can be prepared by different methods such as melt compounding, solution and dispersion blending as well as in-situ polymerization, which is frequently also referred to as ''polymerization filling''. In contrast to highly viscous polymer melts, the polymerization reaction media have much smaller viscosity and enable easy dispersion of nanoparticles, provided that the compatibilities of media and nanoparticles are matched. Moreover, polymerization filling can produce nanocomposites with much higher nanofiller content. This is of interest for masterbatch formation and application as intermediates in melt compounding. There are numerous examples for successful preparation of polyolefin nanocomposites by

* Corresponding author. Tel.: +49 761 203 6270; fax: +49 761 203 6319.
E-mail address: rolf.muelhaupt@makro.uni-freiburg.de (R. Mülhaupt).

0032-3861/$ - see front matter © 2007 Elsevier Ltd. All rights reserved.
doi:10.1016/j.polymer.2007.12.007

polymerization filling. Effective deagglomeration was the key to PE/graphite composites with significant improvement of graphite dispersion with respect to that of melt compounding [8]. In polymerization filling, nanofillers are mostly employed as supports for MAO-activated metallocenes [9]. PE/layered silicate nanocomposites [10,11], PE/graphite composites [12], PE/carbon nanotube nanocomposites [13], iPP/layered silicate nanocomposites [14,15] and sPP/silica monosphere nanocomposites [16] were prepared by means of polymerization filling. Recently Kaminsky et al. have described the synthesis of sPP/carbon nanotubes [17] and iPP/carbon nanotubes nanocomposites [18] and Dubois et al. prepared poly(ethylene-*co*-norbornene) coated carbon nanotubes by means of in-situ polymerization [19]. Especially when the nanofillers are rendered organophilic, this polymerization filling technique represents an attractive ''one-pot'' synthesis towards nanocomposites. In this case organophilic nanofillers are dispersed in the reaction medium and polymerization is carried out in the presence of fillers. This approach has been successfully employed to synthesize HDPE and LDPE/layered silicate nanocomposites [20].

Much less is known concerning the exploitation of organophilic nanoboehmites as nanofillers for polymers [21]. Barron and Obrey prepared organophilic boehmites modified with *p*-hydroxybenzoic acid as components of boehmite-supported catalysts useful in olefin polymerization [22]. In our group, boehmites modified with *p*-toluenesulfonic acid [23,24] and silica doped boehmites [25] were successfully used as supports for olefin polymerization catalysts. The objective of this research was to explore polyethylene–boehmite nanocomposite formation by means of in-situ polymerization. The nanocomposites were formed by performing the metallocene/MAO-catalyzed olefin polymerization in the presence of organophilic boehmites dispersed in the polymerization medium. The influence of boehmites on the polymerization activity of metallocene catalysts and the in-situ formation of nanoboehmite–PE dispersions via deagglomeration of organoboehmite was examined. In addition the influence of in-situ formed nanoboehmites on morphological, thermal and mechanical properties were investigated. An important target was to prepare nanocomposites with very high nanofiller content and uniform nanofiller dispersion as masterbatch component for melt compounding.

2. Experimental

2.1. Materials

All manipulations were carried out under Ar using standard Schlenk and glovebox techniques.

Cp_2ZrCl_2 (98%) was purchased from Aldrich, *rac*-Me_2Si(2-Me-benz[*e*]-Ind)$_2ZrCl_2$ from MCat GmbH, Konstanz, MAO (10 wt.% solution in toluene) from Crompton GmbH, Bergkamen, toluene from Merck, and ethylene (3.0 quality) and argon (5.0 quality) from Air Liquide. The boehmites (trade name Disperal® from Sasol Germany GmbH) used in this study are pseudo-crystalline (crystallite size < 50 nm) and synthesized by a sol–gel route starting from aluminum alkoxides.

Table 1
Properties of Disperal particles

Code	Modification reagent	Modification [wt.%]	Crystallite size [nm]
D	None (neat Disperal)	0	10
DUA2	Undecylenic acid	2	8
DSA2	Stearic acid	2	6
DUA20	Undecylenic acid	20	n.d.
DSA20	Stearic aid	20	n.d.

Data provided by Sasol Germany.

All Disperal samples (Table 1) were generously provided by Sasol Germany, Hamburg. Disperal samples were dried under vacuum at 150 °C for 2 h prior to use. Lupolen 4261A (MFI(190/21.6) = 6 g/10 min) was provided by Basell as polymer powder. Solvents were dried by refluxing over Na/K alloy under inert gas and distilled prior to use.

2.2. Polymerization

Miniclave: The influence of ultrasound dispersion before polymerization was tested in a 200 mL Büchi glass reactor equipped with a mechanical stirrer. Toluene (120 mL) was transferred into the reactor, and 50 mg of DUA2 was dispersed in 20 mL of toluene and treated for 2 min with an ultrasound probe (Bandelin Sonorex) at an amplitude of 60% and transferred into the reactor subsequently. MAO solution (1 mL) was added under stirring. After 30 min, a 5 mL solution of 0.3 mg MBI activated with 1 mL MAO was added. The polymerization was started by applying 2 bar overpressure of ethylene, and the reactor temperature was kept constant at 40 °C by means of a water bath. After a polymerization time of 15 min the reaction was stopped by venting the reactor, the polymer was precipitated in 500 mL methanol acidified with 10 mL of 15 wt.% HCl, and dried at 60 °C under vacuum for at least 18 h.

Multi-purpose polymerization reactor (MPPR): Polymerizations were carried out in an automated 0.6 or 2.0 L double jacket metal reactor which was developed together with Labeq AG, Switzerland. Parameters like reactor temperature, stirrer rotation speed and ethylene pressure were controlled and recorded by a computer. The reactor was filled with toluene and a dispersion of Disperal particles in 20 mL of toluene was added through a pressure lock. One part of the MAO solution was added under stirring and stirring was continued for 30 min. The reactor was saturated with ethylene three times. The catalyst was preactivated with the other part of the MAO solution. The polymerization was started by injecting the activated catalyst solution with a pressure lock after saturation was finished. The reaction was stopped by venting the reactor, the polymer was precipitated in 800 mL methanol acidified with 10 mL of 15 wt.% HCl, and dried at 60 °C under vacuum for 18 h.

2.3. Characterization

Environmental scanning microscopy (ESEM): Samples were sputtered with Au/Pd in a Pollaron Sputter Coater SC 7640.

ESEM images were recorded with an ESEM 2020, Electroscan, Wilmington, USA (5 Torr water vapor atmosphere; acceleration voltage 25 kV). Secondary electrons were detected by a GSED (Gaseous Secondary Electron Detector).

Size exclusion chromatography (SEC): Molecular weights and molecular weight distributions of the polymers were determined using a PL-220 chromatograph (Polymer Laboratories) at 140 °C equipped with three PLGel mixed-bed columns. The solvent used was 1,2,4-trichlorobenzene, stabilized with 2 mg/mL Irganox 1010, at a flow rate of 1 mL/min. PS standards with narrow molecular weight distributions were used for calibration.

Thermal analysis DSC: measurements were carried out on a Seiko 6200 thermal analysis system in the temperature range from −70 to 170 °C at a heating rate of 10 K/min. The second heating curve was used to determine T_m and ΔH_m. TGA measurements were performed on a Netzsch STA 409 in a temperature range form 50 to 650 °C with a heating rate of 10 K/min under N_2 or air atmosphere.

Transmission electron microscopy (TEM): The TEM measurements were carried out with a LEO 912 Omega transmission electron microscope applying an acceleration voltage of 120 keV. The specimens were prepared by melting the polymer particles and subsequently cutting the resulting film in an ultramicrotome (Leica Ultracut UCT) equipped with a cryochamber (Leica EM FCS). Thin sections of about 50 nm were cut with a Diatome diamond knife at −120 °C.

Preparation of test specimens: A Collin 200P vacuum press and a home-made mold was used for compression molding of sheets (2 × 80 × 110 mm). The polymer was stabilized with 0.5 wt.% of a mixture of Irgaphos 168 and Irganox 1010 (1:1) to prevent oxidative and thermal degradations during compression. The polymer powder was filled into the mold, molded for 3 min without pressure at 180 °C and compressed for 3 min at 180 °C and a maximum force of 25 kN and afterwards cooled to 30 °C under compression. From this sheet tensile test specimens according to ISO 527 norm were made with a stamping press. For preparation of samples MC1, MC2 and MC3 PE powder (Lupolen 4261), filler material and 0.1 wt.% stabilizer (Irgaphos 168 and Irganox 1010 (1:4)) were melt blended in a Collin Teachline ZK 25T corotating twin screw extruder at 190–200 °C at a speed of 120 rpm. The obtained strands were pelletized and dried at 80 °C. The different test specimens for tensile strength and notched impact strength were injection molded on a Ferromatic Milacron K40 according to DIN 53455. The temperature of the cylinder was 200–210 °C and the mold was at 60 °C.

Mechanical analysis: Tensile tests were made with a Zwick Z005 machine according to ISO 527. The crosshead speed was 1 mm/min for determination of Young's modulus and 50 mm/min for determination of yield stress and elongation at break. At least five specimens of each sample were measured. Yield stress and Young's modulus were calculated with Zwick Test Xpert software version 11.0 according to ISO 527. Notched impact strength was tested on a Zwick 5102 impact tester (ISO 180/1A).

3. Results and discussion

3.1. Organophilic boehmites

Boehmites $[Al(O)(OH)]_n$ are composed of Al–O double-layers (Fig. 1a) which are interconnected by hydrogen bonds between the hydroxyl groups.

Table 1 summarizes the boehmites used in this study. The crystallite size of the boehmites is in the rage of 10 nm. The boehmites were rendered organophilic by modification with stearic acid and undecylenic acid (Fig. 1b) with a loading of 2 and 20 wt.%, respectively. As a consequence of the modification, these boehmites are easy to disperse in organic media such as toluene. In addition to stearic acid, undecylenic acid was also used as organophilic modifier in order to enable copolymerization of vinyl-functionalized boehmites. The modification with carboxylic acids was performed by Sasol using a process at elevated temperatures described in patent literature [26,27]. An ESEM image of DUA2 displayed in Fig. 2 revealed the size and morphology of the boehmite particles. In the powdery state all boehmite samples form agglomerates of the crystallites with a diameter in the range of 5–50 μm.

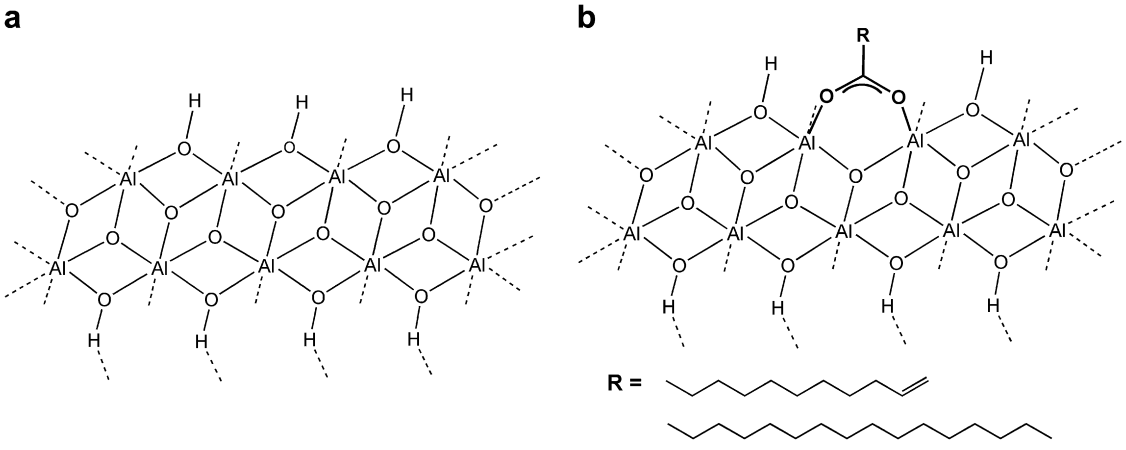

Fig. 1. Structures of (a) pure boehmite and (b) carboxylate-modified boehmite.

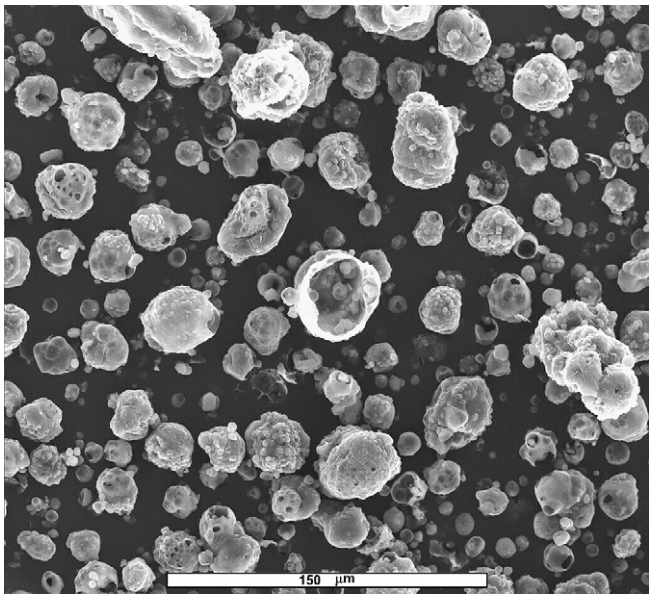

Fig. 2. ESEM image of boehmite modified with 2 wt.% undecylenic acid (DUA2) (scale bar: 150 µm).

3.2. In situ polymerization

Nanocomposites consisting of polyethylene and various boehmites have been prepared by in-situ ethylene polymerization by means of MAO-activated *rac*-Me_2Si(2-Me-benz[*e*]-Ind)$_2ZrCl_2$ (MBI) and Cp_2ZrCl_2 (Cp2) as catalysts. Polymerization conditions and results are listed in Tables 2 and 3. Most of the polymerization reactions were performed in a computer controlled polymerization reactor which allows to control and to monitor parameters like reactor temperature, stirrer speed and ethylene consumption and pressure. All reactions were run until a certain amount of ethylene was consumed.

Prior to polymerization the fillers were dispersed in the reaction medium toluene. MAO was added to the dispersions before catalyst injection in order to deactivate polar groups on the boehmite surface which might be detrimental to the catalyst. After injection of catalyst solution the polymer chains grow in the presence of filler leading to a PE-coating and further fragmentation of the filler particles. Besides the organo-modified boehmites, unmodified boehmite (D) was also used to evaluate the impact of the organic modification on filler dispersion in the polyethylene matrix. For the highly modified boehmites DUA20 and DSA20, stable dispersions are obtained in toluene due to their organophilicity, whereas the unmodified and low-modified boehmites (DUA2 and DSA2) form suspensions.

Fig. 3 compares the polymerization activities in the presence of different fillers at a fixed filler concentration of 5 g/L. In the presence of unmodified and modified boehmite the polymerization activity of Cp2 can be increased. In the presence of 5 g/L DUA2 the polymerization activity of Cp2 is increased by 67%, 5 g/L DSA2 leads to an increase of 53% and 5 g/L D increases the activity by 33%.

One explanation for this observation may be the fact that the boehmite, in particular its hydroxyl groups on the surface, acts a scavenger for free trimethylaluminium (TMA) which is present in commercial MAO solutions and deactivates the active catalyst species. TMA reacts with the hydroxyl groups to produce Al–O–Al species together with the release of methane. It was reported that for the same activity lower aluminum/metal ratios are needed for TMA depleted MAO than for commercial MAO solutions [28,29]. Another reason for the rise in activity might be due to a partial in-situ immobilization of the catalyst on the MAO treated filler surface. Heterogeneous metallocene-catalyzed olefin polymerization needs a considerably lower aluminum/metal ratio than the corresponding homogenous reaction [30]. Thus the polymerization activity is higher in the case of heterogeneous polymerization if the same aluminum/metal ratio is employed. Interestingly, the in-situ formation of the PE nanocomposites leads to millimeter-sized PE particles and prevents reactor fouling which is observed for ethylene polymerization with homogeneous catalysts in the absence of filler. This observation also points towards a partial immobilization of the catalyst.

Table 2
Polymerization conditions and polymer characteristics from in-situ polymerization in the presence of D, DUA2 and DSA2

Run	Catalyst	Filler	[Filler] [g/L]	*t* [min]	Yield [g]	Activity [kg_{PE}/mol_{Zr} h]	M_w [g/mol]	M_w/M_n	T_m [°C]	ΔH_m [mJ/mg]	Filler in polymer [wt.%]
1	Cp2[a]	–	0	108	34.8	1900	463,600	1.9	135.8	171	0
2	Cp2[a]	D	5	45	42.2	5100	510,700	1.9	138.1	155	7
3	Cp2[a]	DUA2	5	32	43.5	7400	509,300	1.9	138	163	7
4	Cp2[a]	DSA2	5	42	43.6	5600	492,500	2.0	137.8	162	7
5	MBI[b]	–	0	71	18.8	16,700	476,700	2.5	136.8	172	0
6	MBI[b]	D	5	32	22.2	40,900	495,000	2.2	135.5	148	7
7	MBI[b]	DUA2	1.7	56	19.1	19,500	428,100	2.2	135	158	3
8	MBI[b]	DUA2	3.3	30	26.8	54,400	456,600	2.4	134.8	158	4
9	MBI[b]	DUA2	5	17	20.8	71,200	463,600	2.2	135.5	161	7
10	MBI[b]	DUA2	10	54	23.7	24,200	n.d.	n.d.	134.3	160	13
11	MBI[b]	DSA2	5	23	22.4	57,400	475,200	2.4	136	163	7
12	MBI[c]	DUA2	61.5	18	76.1	62,900	n.d.	n.d.	132.4	150	53

[a] [Zr] = 17 µmol/L; Al/Zr = 1300; p = 3 bar; V = 650 mL; T = 25 °C.
[b] [Zr] = 3.5 µmol/L; Al/Zr = 5000; p = 3 bar; V = 300 mL; T = 40 °C.
[c] [Zr] = 3.6 µmol/L; Al/Zr = 8300; p = 3 bar; V = 650 mL; T = 40 °C.

Table 3
In-situ polymerization in the presence of DUA20 and DSA20

Run	Filler	[Filler] [g/L]	t [min]	Yield [g]	Activity [kg_{PE}/mol_{Zr} h]	M_w [g/mol]	M_w/M_n	T_m [°C]	ΔH_m [mJ/mg]	Filler in polymer [wt.%]
13	–	0	15	30.8	54,300	535,500	2.8	136.4	161	0
14	DUA20	1.5	23	23.2	26,100	495,400	2.4	134.6	156	4
15	DUA20	3.1	64	24.5	9400	n.d.	n.d.	135.5	143	8
16	DSA20	0.8	9	26.9	80,900	617,200	2.7	134.5	164	2
17	DSA20	1.5	8	27.8	95,300	497,800	2.4	138.8	163	4
18	DSA20	3.1	19	27.5	36,800	n.d.	n.d.	134.4	164	7

Conditions: [MBI] = 3 μmol/L; Al/Zr = 5000; p = 3 bar; V = 650 mL; T = 40 °C.

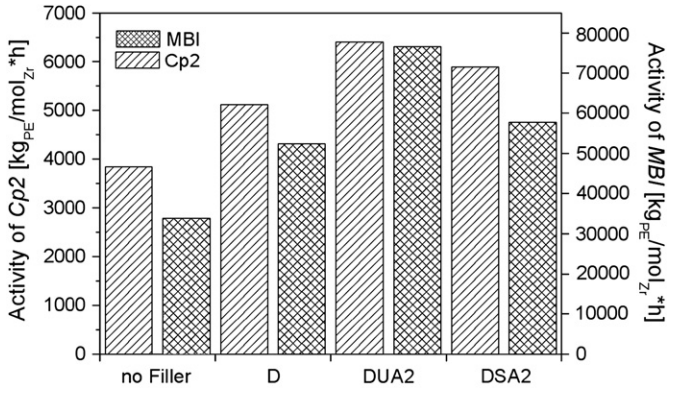

Fig. 3. Polymerization activities of Cp2 and MBI in the presence of boehmite (c(boehmite) = 5 g/L; t_{Pol} = 18 min; conditions: Table 2).

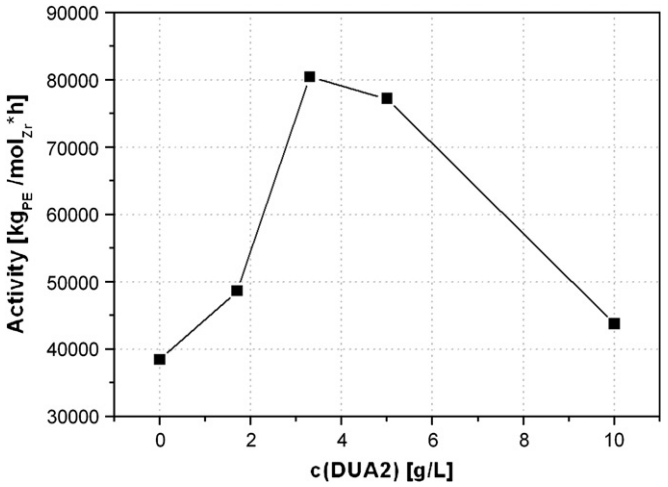

Fig. 4. Polymerization activity of MBI in the presence of different DUA2 concentrations (conditions: Table 2; t_{Pol} = 17 min).

In the case of MBI as catalyst the influence of the filler on the catalyst activity is the same as for Cp2 but the relative increase in activity is more pronounced. In the presence of 5 g/L DUA2 the catalyst activity is doubled, in the case of D and DSA2 it is increased by 50 and 70%, respectively. But like Cp2 the presence of DUA2 results in the highest activity followed by DSA2 and D.

In the system MBI/MAO and DUA2 the influence of different filler concentrations was investigated. The filler concentration was varied within 0 and 10 g/L (Fig. 4). A concentration of 3.3 g/L seems to be an optimal concentration in terms of activity. At this concentration catalyst activity is 2.1 times higher than in the absence of filler. When going to higher filler concentrations catalyst activity decreases but at a concentration of 10 g/L it is still higher than the polymerization activity in the absence of filler.

The stabilizing effect of the filler on polymerization activity can also be seen by investigating the polymerization kinetics with a mass flow meter. Fig. 5 shows the profile of polymerization activity for a homogeneous polymerization and for a polymerization in the presence of 3.3 g/L DUA2. Without filler the activity decreases a few minutes after starting the polymerization. In the presence of filler the activity remains above the initial activity and the activity without DUA2 particles during the first 25 min of the reaction indicating improved catalyst stability or a better ethylene diffusion due to a partial heterogenization of the catalyst. The influence of very high DUA2 concentrations (61.5 g/L; run 12) on polymerization activity was also investigated. This technology is attractive to produce highly filled masterbatches which can be employed in melt compounding to facilitate nanoparticle dispersion in highly viscous media typical in melt processing. In contrast to many other polymerization filling approaches it was quite surprising that the high concentrations of organoboehmite did not cause catalyst poisoning. Polyethylene containing 53 wt.% DUA2 could be synthesized in good yield.

The influence of particles with a high organic modification (DUA20, DSA20) on the polymerization activity of MBI was

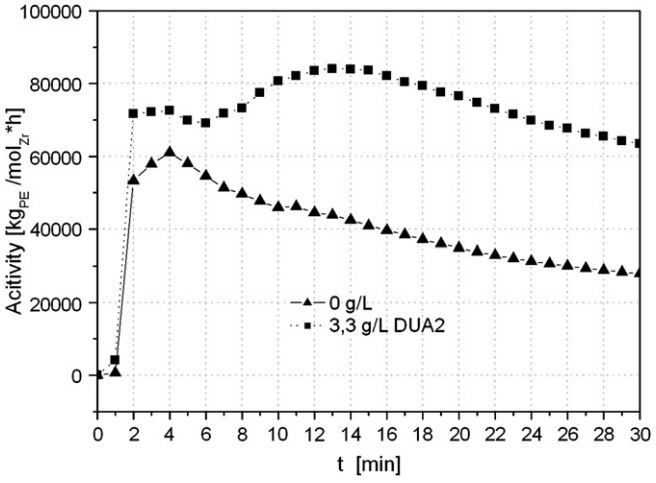

Fig. 5. Polymerization kinetic of MBI without filler and in the presence of 3.3 g/L DUA2 (conditions: [MBI] = 3.5 μmol/L; Al/Zr = 5000; T = 40 °C; p = 3 bar).

also investigated. As it can be seen from Fig. 6 up to a concentration of 1.5 g/L of DUA20 and DSA20 the catalyst activity can be enhanced. In the case of 1.5 g/L DSA20 the activity increased by 100% and reaches its maximum at this concentration. In the case of 1.5 g/L DUA20 the activity is only enhanced by 20%. When increasing the filler concentration to 3 g/L catalyst activity rapidly decreases. These observations are in contrast to the experiments with DUA2 and DSA2 in which DUA2 gave the highest activity at a concentration of 3 g/L. An explanation could be that the high loading of carboxylic acids on the particles deactivates the catalyst by poisoning it with ester functionalities. A hypothesis to interpret the higher activity in the case of stearic acid modified particles might be that the catalyst poisoning ester group on the particle surface is better shielded by stearic acid which possesses a longer alkyl chain (C_{18}) than undecylenic acid (C_{11}).

The filler content achieved by the in-situ polymerization process was determined by means of thermogravimetric analysis (TGA). Fig. 7 shows representative TGA traces of some composites. It can be seen that the filler material does not influence the degradation temperature of the PE matrix. Neat PE, hybrid materials of PE and unmodified fillers (D, run 6), fillers with low organic modification (DSA2, run 7) and with high amount of modifier (DSA20, run 16 and 17) degrade at 450 °C under nitrogen. The recovered mass of the composites after the thermal degradation does not show a significant difference between the measured and the theoretical filler content. The composites with D and DSA2 should have 7 wt.% of inorganic filler which is almost identical with the measured filler content of 6.5 wt.%. In the case of DSA20 (runs 17 and 18) the theoretical amount of inorganic residue should be 3.2 and 5.5 wt.% and was verified experimentally to be 3.8 and 5 wt.%. According to this observation it is obvious that all the boehmite dispersed in the reactor is incorporated during the polymerization process. In addition, TGA measurements under air were made to study if the filler influences the oxidative degradation of the polymer (Fig. 8). It could be shown that neither filler with low organic modification (DSA2) nor filler

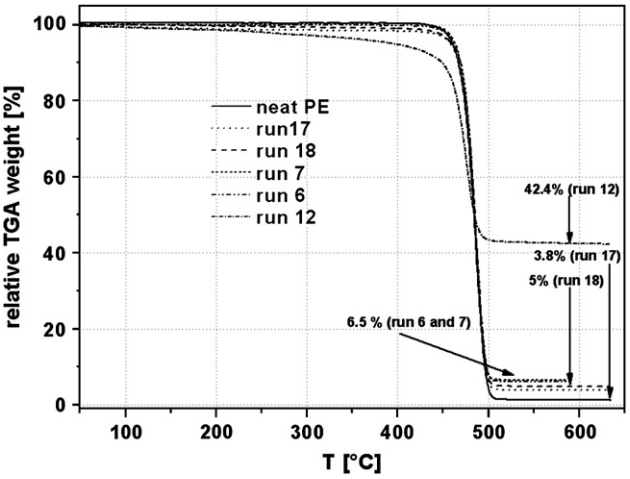

Fig. 7. TGA traces of some nanocomposites compared with pure PE (N_2 atmosphere).

with high amount of organic modification (DSA20) accelerates oxidative degradation of the PE matrix. The degradation starts at 250 °C; at 400 °C a sharp weight loss for all samples are observed.

Within the range of the prepared catalyst families, polymer molar masses and polydispersities were not affected by the presence of fillers during the polymerization. M_w is in the range of 428,100–617,200 and the polydispersity lies between 2 and 3. This is of particular interest when examining the mechanical properties of the composite materials meaning that effects observed are related to the filler and not related to a change in polymer properties. According to DSC measurements the fillers do not have a great influence on the melting temperature. In series with Cp2 as catalyst the melting temperatures are slightly shifted to higher values for the filled polymers. In the series with MBI no trend in melting temperatures can be seen. For all filled polymers a small loss of crystallinity can be detected which is observable in the reduction of ΔH_m (Tables 2 and 3). Only in the case of DSA20 ΔH_m values are not reduced but are almost the same than that of the neat PE.

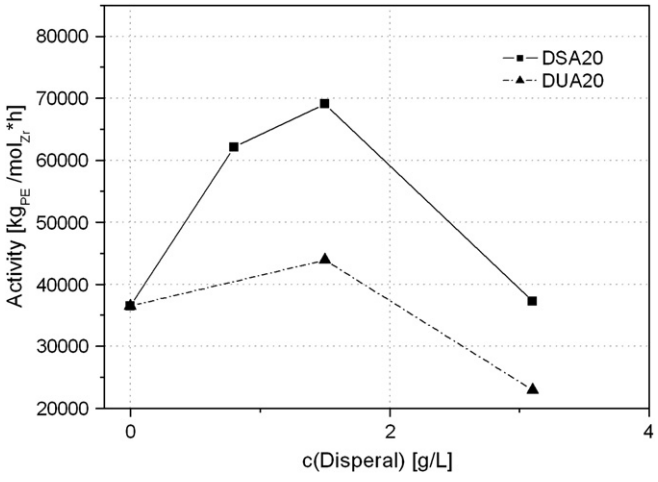

Fig. 6. Polymerization activity of MBI in the presence of different DUA20 and DSA20 concentrations (conditions: Table 3; $t_{Pol} = 8$ min).

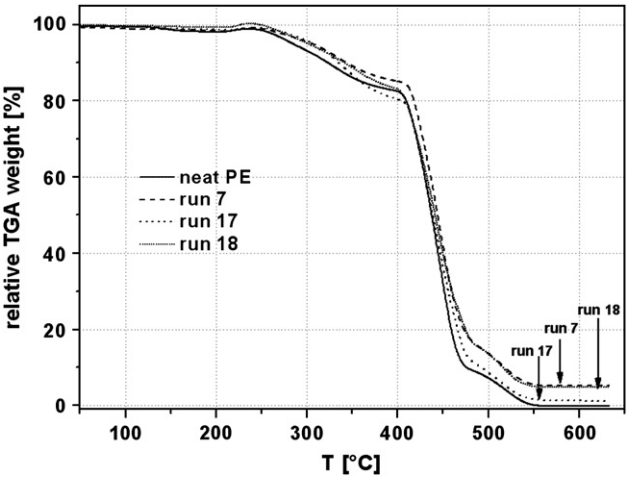

Fig. 8. Oxidative degradation of some nanocomposites compared with pure PE (TGA under air atmosphere).

3.3. Morphological properties

The PE/boehmite powders from the reactor were compression molded to produce sheets (cf. Section 2). Inspection of these sheets showed that the boehmite fillers did not affect the visual properties of the polymer compared to the neat PE sheets. Neither samples with unmodified, low modified nor highly modified Disperal showed any coloring or visible inhomogeneities. To examine the dispersion of the nanoparticles within the polymer matrix TEM images were recorded after cutting slides out of the samples by ultra-microtomy at −130 °C. Fig. 9a shows a TEM image of a composite with 7 wt.% unmodified boehmite D. The picture shows large aggregates of boehmite particles. One can see that these aggregates are composed of nanometer sized particles. Few nanoparticles can be found between these agglomerates. In the case of D as filler material the interactions between the individual filler nanoparticles seem to be too strong to be broken up during the in-situ polymerization process. These interactions are mainly hydrogen bonds between the OH groups on the particle. A method to break up these aggregates by polymerization might be the immobilization of the metallocene/MAO system on the boehmite surface as described by Barron and Obrey [22]. Results on this research will be published in detail shortly. As shown in Fig. 9b fillers rendered organophilic with 2 wt.% stearic acid do not form such large aggregates. A modification with 2 wt.% carboxylic acid reduces the size of the aggregates from several micrometers to about 500 nm but cannot reduce the filler–filler interaction to enable complete deagglomeration. Composites with DUA2 as filler reveal the same properties in terms of cluster size and particle dispersion. In addition, the role of ultrasound with respect to facilitating the deagglomeration of DUA2 particles was investigated. The toluene DUA2 dispersion was subjected to ultrasound treatment before starting the in-situ polymerization. As seen in Fig. 10a, ultrasound treatment prior to the polymerization cannot completely break up the boehmite clusters. But at least in some areas of the polymer a fine dispersion of the DUA2 particles (Fig. 10b) was observed after ultrasound treatment.

In order to find out how to improve the dispersion of organophilic boehmite fillers in the polymer matrix the organophilic modification was increased drastically by immobilizing 20 wt.% of stearic acid and undecylenic acid on the particles (DUA20, DSA20). Again TEM investigations of composites with these fillers were made (Fig. 11). In contrast to D, DSA2 and DUA2 the highly modified fillers afford very uniformly dispersed boehmite particles with particle sizes between 50 and 100 nm. No agglomeration above 200 nm was observed either for DUA20 or for DSA20 as fillers. Due to these observations it can be shown that increasing amount of organic modifier improves the dispersion of the filler in the polymer matrix. The organic modifier can be regarded as a kind of compatibilizer between polar filler particles and nonpolar PE matrix thus improving the filler dispersion. Additionally the organic modification reduces particle–particle interactions caused by hydrogen bonds between surface OH groups.

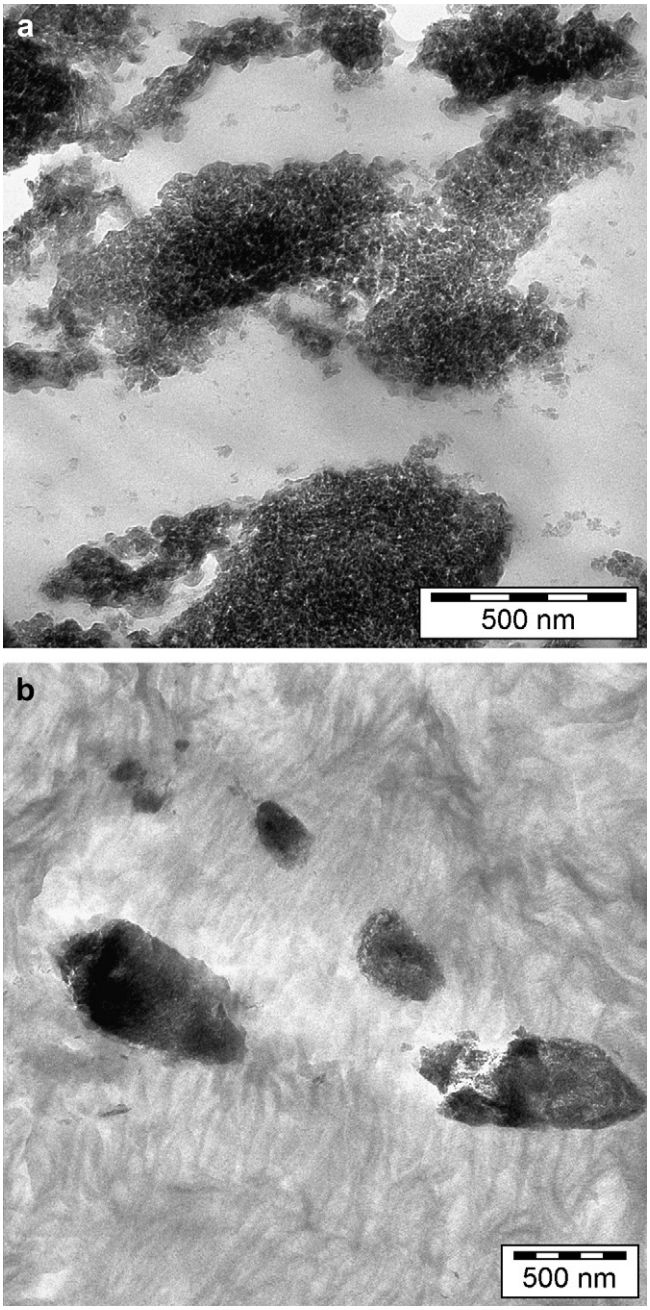

Fig. 9. TEM images of PE–boehmite nanocomposites: (a) 7 wt.% D and (b) 7 wt.% DSA2.

3.4. Mechanical properties

The mechanical properties of the boehmite–PE hybrid materials were investigated by tensile testing experiments. The data of the tensile testing experiments is summarized in Table 4. First samples with the same filler concentration (7 wt.%) were tested to compare the effects of the different fillers. In the series with CP2 as catalyst (runs 1–4) the Young's modulus of all filled materials was increased (Table 4). For example, DSA2 addition increased Young's modulus from 800 (neat PE) to 920 MPa, which is an improvement of 16%. D as filler can increase the Young's modulus by 60 MPa followed by DUA2

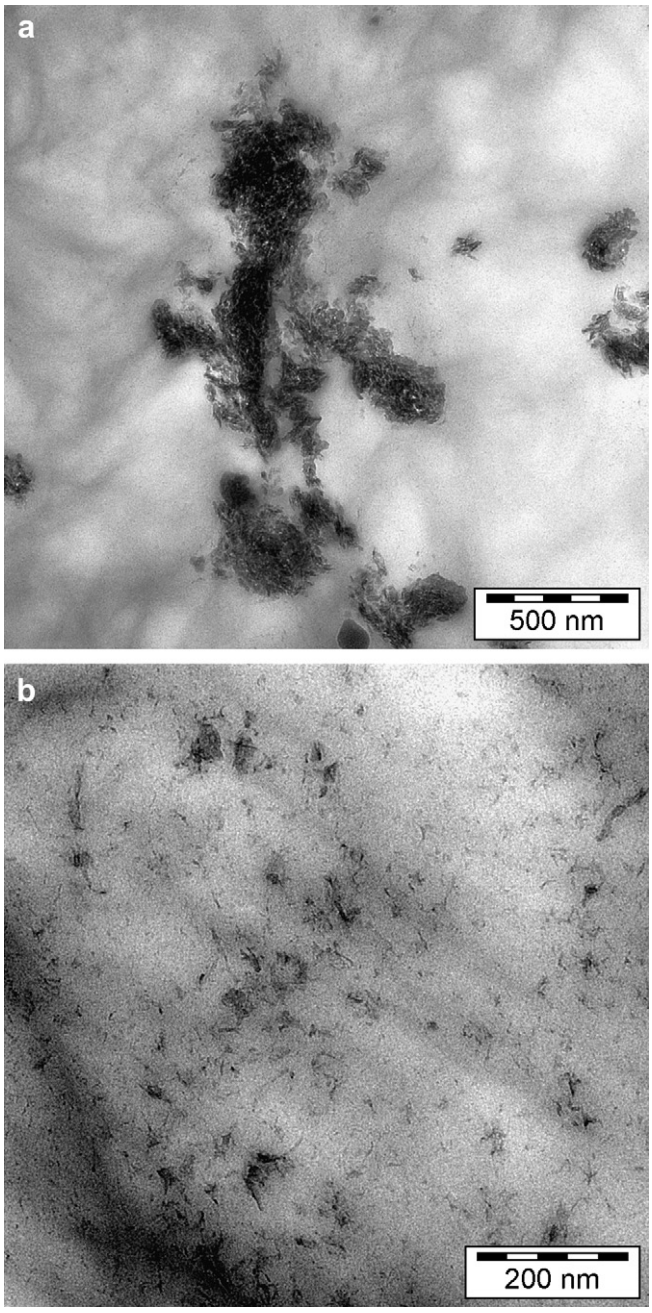

Fig. 10. (a) TEM of PE–DUA2 composite synthesized by in-situ polymerization after treatment of the toluene DUA2 dispersion with an ultrasound probe and (b) area with homogeneous filler dispersion.

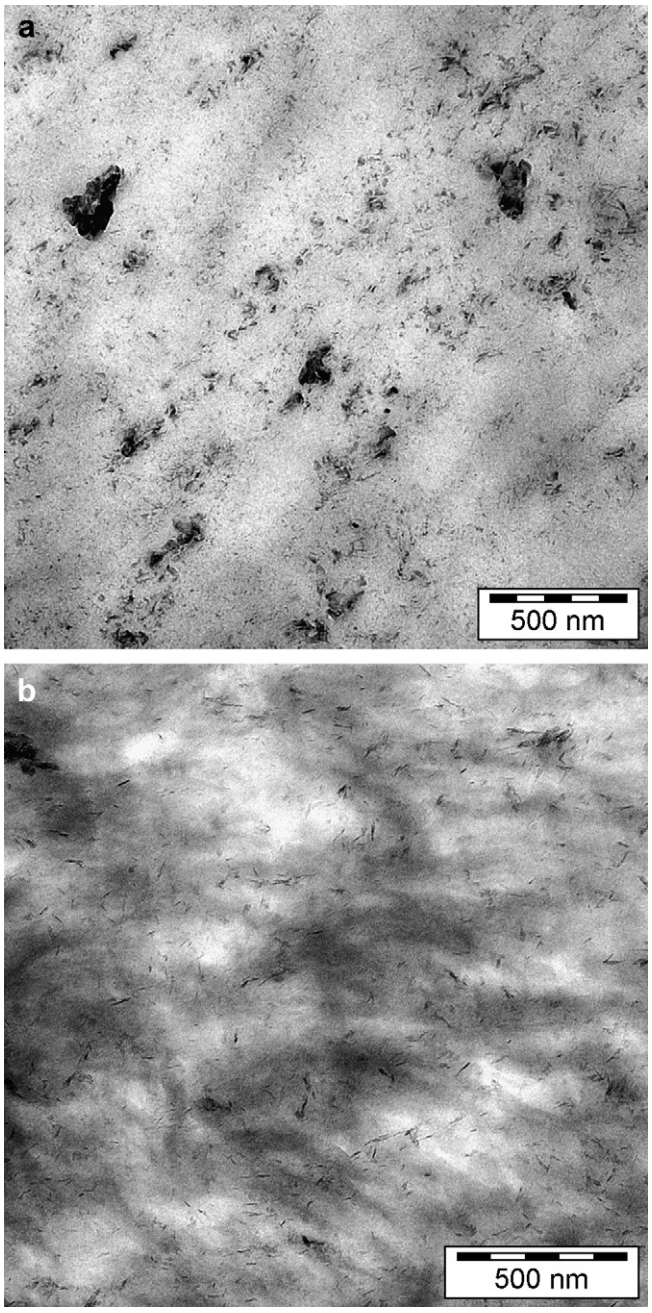

Fig. 11. TEM images of (a) PE–DUA20 (run 18) and (b) PE–DSA20 nanocomposites (run 16).

with an increase of 40 MPa. Interestingly no decrease in elongation at break can be observed. Often inorganic fillers increase the stiffness at the expense of elongation at break.

In the series with MBI as catalyst (runs 5, 6, 9, and 11) the reinforcement effects were not so pronounced as in runs 1–4. But also in this series DSA2 gave the highest increase in stiffness without a significant reduction of elongation at break. The matrix reinforcement at 7 wt.% organoboehmite is lower with respect to organoclays. This can be attributed to the low aspect ratio of the organoboehmites used in this investigation.

The influence of highly modified Disperal particles (DSA20 and DUA20) on the mechanical properties was also investigated. This is of particular interest as these filler materials gave a homogeneous and nanometer sized dispersion. With filler content of 4 wt.% of DSA20 the Young's modulus was increased by 70 MPa; when increasing the filler content to 7% an increase in stiffness of 110 MPa, equivalent to 14%, is achieved. As shown in Fig. 12 there is a linear relation between Young's modulus and filler content. As shown before stearic acid modification leads to better mechanical properties than modification with undecylenic acid. DSA20 of 4 wt.% reduces the elongation at break but a further increase in filler concentration to 7 wt.% does not lower the elongation at break significantly more. Compared to the sample with 7 wt.%

Table 4
Mechanical properties of the nanocomposites prepared by in-situ polymerization

Run	Filler [wt.%]	Young's modulus [MPa]	Yield stress [MPa]	Elongation at break [%]
1	–	800 ± 10	19 ± 0.1	240 ± 44
2	7% D	860 ± 15	19.2 ± 0.2	220 ± 35
3	7% DUA2	830 ± 16	19.3 ± 0.2	250 ± 13
4	7% DSA2	920 ± 23	19.2 ± 0.2	230 ± 11
5	–	800 ± 19	19.7 ± 0.3	360 ± 41
6	7% D	840 ± 19	19.2 ± 0.3	290 ± 53
9	7% DUA2	820 ± 22	18.9 ± 0.2	240 ± 34
11	7% DSA2	860 ± 39	19 ± 0.3	310 ± 24
13	–	790 ± 22	19.5 ± 0.3	250 ± 61
15	8% DUA20	840 ± 22	18.9 ± 0.5	270 ± 144
17	4% DSA20	860 ± 16	19.7 ± 0.2	150 ± 69
18	7% DSA20	900 ± 18	19.9 ± 0.2	150 ± 12

DSA2 (run 11), 4 wt.% DSA20 (run 17) gives the same performance in terms of stiffness. This might be a result of the fine dispersion of the filler particles in the polyethylene matrix.

The nanocomposite containing 52 wt.% organoboehmite DUA2 (run 12) was used as a masterbatch in PE melt extrusion adding neat HDPE (Lupolen 4261A) as diluent to produce PE nanocomposites with 7 wt.% organoboehmite content (MC3). The mechanical properties of this compound are listed in Table 5. Fig. 13 compares the properties of PE nanocomposites prepared by means of melt extruding PE and neat DUA2 (MC2) and by means of melt extruding the in-situ masterbatch (MC3). In contrast to conventional melt processing (MC2) the in-situ masterbatch afforded much higher stiffness and yield stress. In the case of MC2 Young's modulus is increased by only 3% whereas in the case of MC3 an increase of almost 30% is observed. This is attributed to the improved dispersion when masterbatches are produced by in-situ polymerization.

4. Conclusion

Metallocene/MAO-catalyzed ethylene polymerization in the presence of organoboehmites, which were rendered organophilic by means of modification with undecylenic and stearic acid, led to the formation of new families of boehmite-based polyolefin nanocomposites. The dispersion of the organoboehmites was controlled by the amount of carboxylate on the boehmite surface. Organoboehmites containing 2 wt.% carboxylic acid modification showed an improved dispersion in the PE matrix compared to unmodified boehmites. However, the fillers still agglomerated to form clusters of about 500 nm. In contrast, the organoboehmites containing 20 wt.% carboxylic acid modification were uniformly dispersed in the polymer matrix showing agglomerate sizes below 100 nm.

Both unmodified boehmites and organoboehmites containing 2 wt.% organic modification increased the catalytic activity of the MAO-activated metallocenes used in this study. Even at filler concentrations of 10 g/L catalytic activity was higher than that in the absence of boehmite. This observation may be explained by the ability of the boehmite particles to act as a scavenger for free trimethylaluminium which deactivates the active catalyst species. The elimination of free trimethylaluminium occurs via its rapid reaction with surface hydroxyl groups to produce Al–O–Al species and methane. At the larger content of 20 wt.% carboxylate, the increased content of the ester donor appeared to adversely affect polymerization especially when exceeding 1.5 g/L concentration. The evaluation of mechanical properties revealed that in-situ polymerization gave much improved organoboehmite dispersion and improved stiffness without encountering drastic losses of elongation at break. Since this polymerization filling technology enables the production of nanocomposites with nanofiller content exceeding 50 wt.%, it can be used to produce masterbatches of organoboehmite for melt compounding application. Melt extrusion of such masterbatches resulted in improved mechanical properties.

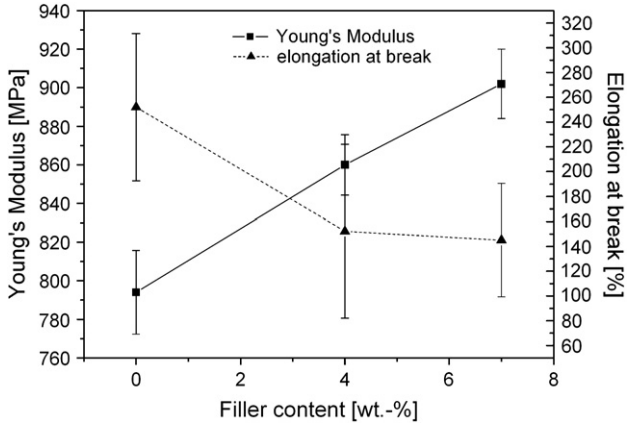

Fig. 12. Mechanical properties of PE–DSA20 nanocomposites at various filler concentrations.

Table 5
Mechanical properties of the nanocomposites prepared by melt compounding

Run	Filler [wt.%]	Young's modulus [MPa]	Yield stress [MPa]	Elongation at break [%]	Impact strength Izod [kJ/m^2]
MC1	–	790 ± 24	29.2 ± 0.6	20 ± 3.1	55.4 ± 1.7
MC2	7% DUA2	810 ± 35	30.2 ± 0.3	20 ± 4.3	38 ± 1.4
MC3	7% DUA2 (run 12)	1020 ± 57	34.7 ± 2.2	15 ± 1.5	46.3 ± 3.5

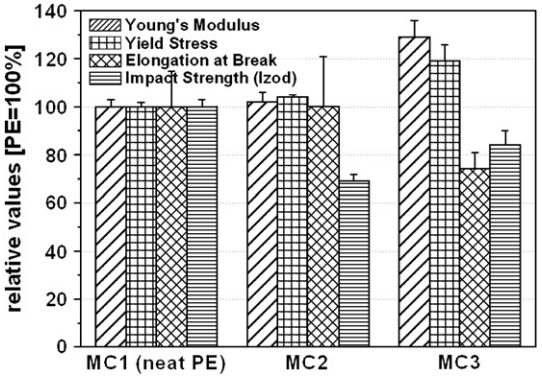

Fig. 13. Comparison of melt compounded PE (MC1) with melt compounded PE together with 7 wt.% DUA2 (MC2) and with melt compounded PE mixture with PE–DUA2 masterbatch (MC3).

Acknowledgements

The authors would like to thank the European Union for financial support (FP6 Project: NMP3-CT-2005-516972) and Olaf Torno of Sasol Germany GmbH (Hamburg) for the fruitful cooperation and supplying us with Disperal samples. We would especially like to thank Dr. Yi Thomann for recording the TEM images, Rainer Wissert for recording the ESEM images and Rouven Streller for help with the extrusion experiments. The technical assistance of Andreas Warmbold and Melanie Strecker is gratefully acknowledged.

References

[1] Mülhaupt R. Kunststoffe 2004;94(8):76–88.
[2] Gilman JW. Appl Clay Sci 1999;15:31–49.
[3] Zanetti M, Kashiwagi T, Falqui L, Camino G. Chem Mater 2002;14(2):881–7.
[4] Mülhaupt R, Engelhardt T, Schall N. Kunststoffe 2001;91(10):178–90.
[5] Gorrasi G, Tortora M, Vittoria V, Kaempfer D, Mülhaupt R. Polymer 2003;44(13):3679–85.
[6] Bauer F, Flyunt R, Czihal K, Buchmeiser MR, Langguth H, Mehnert R. Macromol Mater Eng 2006;291(5):493–8.
[7] Vaia RA, Vasudevan S, Krawiec W, Scanlon LG, Giannelis EP. Adv Mater 1995;7(2):154–6.
[8] Pluta M, Alexandre M, Blacher S, Dubois P, Jérôme R. Polymer 2001;42(22):9293–300.
[9] Alexandre M, Martin E, Dubois P, Garcia-Marti M, Jérôme R. Macromol Rapid Commun 2000;21(13):931–6.
[10] Alexandre M, Dubois P, Sun T, Garces JM, Jerome R. Polymer 2002;43(8):2123–32.
[11] Bergman JS, Chen H, Giannelis EP, Thomas MG, Coates GW. Chem Commun 1999:2179–80.
[12] Alexandre M, Pluta M, Dubois P, Jérôme R. Macromol Chem Phys 2001;202(11):2239–46.
[13] Bonduel D, Mainil M, Alexandre M, Monteverde F, Dubois P. Chem Commun 2005:781–3.
[14] Ma J, Qi Z, Hu Y. J Appl Polym Sci 2001;82(14):3611–7.
[15] Sun T, Garcés JM. Adv Mater 2002;14(2):128–30.
[16] Kaminsky W, Funck A, Wiemann K. Macromol Symp 2006;239(1):1–6.
[17] Wiemann K, Kaminsky W, Gojny FH, Schulte K. Macromol Chem Phys 2005;206(15):1472–8.
[18] Funck A, Kaminsky W. Compos Sci Technol 2007;67(5):906–15.
[19] Bredeau S, Boggioni L, Bertini F, Tritto I, Monteverde F, Alexandre M, et al. Macromol Rapid Commun 2007;28(7):822–7.
[20] Heinemann J, Reichert P, Thomann R, Mülhaupt R. Macromol Rapid Commun 1999;20(8):423–30.
[21] Adhikari R, Henning S, Lebek W, Godehardt R, Ilisch S, Michler GH. Macromol Symp 2006;231(1):116–24.
[22] Obrey SJ, Barron AR. Macromolecules 2002;35(5):1499–503.
[23] Xalter R, Halbach TS, Mülhaupt R. Macromol Symp 2006;236(1):145–50.
[24] Xalter R, Mülhaupt R. Polym Mater Sci Eng 2006;94:477–8.
[25] Xalter R, Mülhaupt R. Polym Mater Sci Eng 2006;94:612–3.
[26] Hurlburt PK, Plummer DT (inventors). Condea Vista Company. U.S. Patent 6,227,846; 2001.
[27] Leach BE, Decker LB (inventors). Vista Chemical Company. U.S. Patent 4,676,928; 1987.
[28] Pédeutour J-N, Radhakrishnan K, Cramail H, Deffieux A. J Mol Catal A Chem 2002;185(1–2):119–25.
[29] Pédeutour J-N, Radhakrishnan K, Cramail H, Deffieux A. Polym Int 2002;51(10):973–7.
[30] Hlatky GG. Chem Rev 2000;100(4):1347–76.